Electrostriction in the semiconductor-to-metal transition of liquid Se-Te alloys

Melvin Cutler, Shaw Shya Kao, and Larry A. Silva
Department of Physics, Oregon State University, Corvallis, Oregon 97331-6507
(Received 21 August 1989)

The decrease in atomic volume which accompanies the electronic changes in the semiconductor-metal transition is explained by local compression of the dielectric fluid in the vicinity of negative ions, caused by the attractive force of the electric field on the polarizable atoms. A thermodynamic expression is derived which relates the atomic volume to the mean-square electric field in terms of the macroscopic polarizability and compressibility. The error due to the use of macroscopic parameters on an atomic scale of distance is found to be corrected by a term containing a single empirically determined parameter. This makes it possible to calculate volume changes from experimentally determined negative-ion concentrations which agree with experiment. Near the beginning of the semiconductor-metal transition, where it cannot be inferred from electronic data, information about the negative-ion concentrations is derived from the experimental volume contraction by the use of the model. The semiconductor-metal transition is caused by rapid thermal generation of negative ions, and we trace this to the strong electronic screening of the negative ions by holes, which occurs when the Fermi energy shifts into the valence band.

I. INTRODUCTION

There has long been a considerable interest in liquid binary alloys Se_xTe_{100-x} as systems that may exhibit a metal-insulator (or metal-semiconductor) transition.[1-3] Selenium is a liquid semiconductor with a very small conductivity which increases rapidly with increasing temperature. Tellurium is beneath Se in the Periodic Table, and is chemically similar to Se but more metallic. Molten Te is a poorly conducting metal, that is, its conductivity is many orders of magnitude greater than in Se, and the temperature coefficient is relatively small. In the alloys Se_xTe_{100-x}, the curves for the conductivity versus temperature T show a smooth progression from semiconducting to metallic behavior as x decreases.[1] The transition to the metallic state occurs roughly in the range of x values between 50 and 30. A similar continuous change is found in the other electronic properties: the thermoelectric power,[1] magnetic susceptibility,[4] and the optical absorption.[5]

Interest in this semiconductor-metal transition has been stimulated by the observation of anomalies in the thermochemical properties of the alloy. In the same range of x and T as the semiconductor-metal transition, the coefficient of thermal expansion becomes negative,[6] the compressibility decreases with increasing T,[7] and the heat capacity goes through a maximum.[8] These anomalies have the appearance of a phase change which is spread out over a range of temperature (about 200 K), and the change can be described, with certain limitations, in terms of an equilibrium between a low-temperature and a high-temperature form of the liquid.[9]

Attempts to explain the behavior of Se_xTe_{100-x} have relied strongly on the structural information derived from diffraction studies. Both Se and Te form trigonal crystalline solids which correspond to stacked chains of twofold (2F) covalently bonded atoms. In the molten state, the diffraction information for Se and Se-rich alloys is consistent with the preservation of the 2F coordination in chainlike molecules with a random arrangement of Se and Te atoms in the chains.[10] Other considerations lead to the belief that increasing concentrations of bond defect atoms are thermally generated as T is increased or as x is decreased, which terminate the chains if they are 1F (onefold bonding) and create chain branches if they are 3F (threefold bonding).[3,4,11] The principal bond defects are believed to be negative 1F ions (D^-), positive 3F ions (D^+), and neutral 1F dangling-bond atoms (D^*). There is much more uncertainty about the structure of Te-rich alloys and molten Te. Early diffraction studies by Tourand and co-workers indicated that the coordination number near the melting point of Te is about 3, and increases at higher temperatures.[12,13] Because of the presence of two atomic species, the interpretation of diffraction data for the alloys is more uncertain. But it suggests that a change in structure to one approaching pure Te occurs in the alloys, which first becomes visible at $x < 50$.[10] Recently, Raman scattering measurements have been made which show a qualitative change in bond coordination from one that characterizes Se, at $x \geq 30$, to one that characterizes Te, at $x \leq 20$.[14,15]

The evidence that liquid Te has a threefold coordination number has led Cabane and Friedel to suggest that the atoms in liquid Te have 3F bonding similar to arsenic.[16] A basic difficulty with this interpretation is that when a group-VI element such as Te or Se forms a 3F covalent bond, the Fermi energy can be expected to be near the bottom of the conduction band, whereas the observed electrical behavior of Se_xTe_{100-x} indicates that the Fermi energy is in the band gap or near the top of the valence band.[2,17]

Other models for the behavior of the Te-rich alloys as-

sume that the metallic behavior is associated with the threefold coordination which is believed to occur in Te. In the models advanced by several groups, this metallic behavior of Te is combined with the semiconductor behavior of Se or a Se-rich alloy through the mechanism of microscopic heterogeneity.[18–20] That is, it is assumed that the atoms form clusters of two kinds (or more), one of which has the electrical and thermochemical properties of a metal, and the other has the properties of a semiconductor. There are basic objections to models that depend on microscopic heterogeneity. These include the neglect of surface forces, and the small composition fluctuations predicted theoretically from thermochemical data, both of which would make such a structure unstable. Very recently, optical-absorption measurements have been made for Se_xTe_{100-x} which seem to directly contradict the hypothesis of microscopic heterogeneity.[5]

One of the motivations for heterogeneous models is that they provide an easy explanation of the transport data. A recent analytical study of transport data for Se_xTe_{100-x} in the metallic range $x<50$ has led to a coherent interpretation of the electronic structure in terms of conventional concepts for the electronic behavior of a disordered homogeneous system.[17] It shows that as the transition from semiconductor to metallic behavior develops, the Fermi energy E_F moves from the bottom of the band gap into the valence band, and quantitative information is derived about the shape of the valence band, the hole concentration, and the position of E_F as a function of x and T. The results also indicate that this process is accompanied by merging with the valence band of an acceptor band whose empty and filled states correspond to D^* and D^- centers. This occurs at compositions $x=30$–40. This seems to provide a basis for understanding the electronic transition.

The thermodynamic transition can be interpreted by a chemical model in terms of chemical equilibrium between a low-temperature and a high-temperature form of the liquid. At a given composition, the temperatures which characterize the thermodynamic transition correlate extremely well with the temperatures for the electronic transition.[9] This leads to the key question: What is the mechanism that links the electronic aspects with the thermochemical aspects of the transition?

It seems hard to reconcile the molecular implications of the electronic behavior in the metal transition with an increase in the coordination number which has been supposed to cause the atomic volume decrease. In Fig. 1, we show the hole concentration h^+ as a function of temperature derived in Ref. 17. (All concentrations are normalized to the concentration of atoms N_a, which is assumed nominally to be 2.7×10^{22} cm^{-1}.) The requirement of charge neutrality implies that the concentration d^-, of 1F negative ions is at least as large as h^+, so that the concentration of 1F atoms exceeds 50% at the metallic end of the transition. This should result in an average coordination number at small x and large T which is smaller than 2, rather than larger, as is commonly believed.

A concept which might resolve this conflict is that a 1F bond defect atom can bind to a neighboring 2F (twofold bonded) atom, to form a 3F center.[21] This reaction is

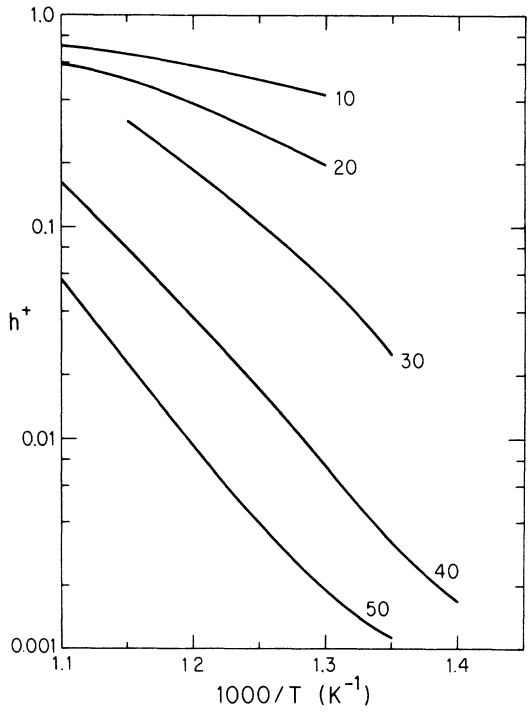

FIG. 1. Concentrations of holes as a function of T at various compositions x, determined in Ref. 17.

normally inhibited energetically because the extra electrons in the broken-bond orbitals have to be promoted into the higher-energy conduction band. It has been widely believed, however, that the transition to the metallic state is accompanied by a smearing of the band gap, which could give rise to conduction-band states below the Fermi energy E_F due to overlap of states of the conduction and valence bands. In that case, one could conceive of a model in which the D^- ions transform into 3F centers in the metallic situation.

We have recently completed an experimental study of the optical absorption and reflectivity of liquid Se-Te, one of whose goals was to obtain quantitative information about the behavior of the band gap in the course of the metal transition.[5] A striking result of this study is evidence that the gap between the conduction-band edge and the highest filled state of the valence band is always positive, even at the composition $x=0$. Furthermore, there is no visible evidence of a distortion of the shape of the density of states near the band edges which one might expect from a secondary bonding interaction between the D^- ions and neighboring 2F atoms.

These results seem to contradict models which convert 1F bond defect centers into 3F centers, and force us to seek an explanation for the structural and thermodynamic information in terms of the formation of 1F D^- ions in the course of the metal transition. On considering the interactions between a D^- ion and its neighboring atoms, it becomes apparent that the attraction of the polarizable neutral atoms on other chains close to an ion will create a local pressure that will appreciably compress the liquid in the vicinity of the ions. Also, it appears to us that this

phenomenon can cause changes in the pair distribution function and the character of the vibration modes which are consistent with the observed diffraction and Raman scattering data.

The purpose of this paper is to develop an explanation for the semiconductor-to-metal transition in terms of electrostriction. This is done by relating the electronic information about the concentration of ions to the thermodynamic information about the change in volume as a function of composition and temperature. In Sec. II, a basic relationship is derived which relates the microscopic change in volume to the compressibility, the dielectric constant, and the change in the magnitude of the microscopic electric field. In order to use this relation, it is necessary to determine the charge distributions and fields near the ions. This is done in Sec. III with the help of approximate models. For alloys at high Te concentrations and at high T, it is possible to derive the volume contraction from the experimentally determined values of $\mathcal{N}^+$. But near the semiconductor side of the transition, the concentration $\mathcal{N}^+$ of positively charged 3F ions is comparable to $\mathcal{N}^+$, and there is insufficient information to determine the ion concentrations. In this case, we use the experimental information about the volume contraction to derive information about the ion concentrations as a function of T and x. In Sec. IV, we discuss the enhanced rate of thermal generation of negative ions which underlies the metal transition, and examine the role of electronic screening in this process. Finally, in the last section, we discuss the limitations of our results which arise from the use of macroscopic concepts in a domain where the microscopic details of the atomic structure are important. We also discuss the compatibility of our model with existing structural information about Se-Te alloys.

II. THERMODYNAMIC BASIS OF ELECTROSTRICTION

A. Phenomenological relations

Though not a very commonplace phenomenon, electrostriction is often a significant factor in the behavior of aqueous electrolyte solutions.[22] Its presence is revealed in the small partial molar volumes of the ions, which may be even negative for the smaller positive ions. The polarization of water involves orientation of the solvent molecules by the electric field, and may therefore be sensitive to temperature. In the case of liquid Se-Te, which does not have large permanent dipoles, this complication does not occur.

We shall describe electrostriction in liquid Se-Te in terms of a thermodynamic theory for a dielectric fluid in an inhomogeneous electric field. This results in equations which, strictly speaking, are invalid when applied to microscopic regions in the immediate vicinity of ions, but it turns out that much of the ensuing error can be corrected by adding a simple empirically derived term. The equation of state includes the polarization $\mathbf{P}$ and the electric field $\mathcal{E}$ in addition to the usual pressure p, volume V, and temperature T. The differential work contains a term involving $\mathbf{P}$ and $\mathcal{E}$ in addition to the $p\,dV$ term. For a chemically homogeneous system in which the number of particles, N, is a variable, the first law of thermodynamics gives

$$dU = T\,dS - p\,dV + \mathcal{E}\cdot d\mathbf{P} + \mu\,dN\ , \tag{1}$$

where U is the internal energy, μ is the chemical potential, and S is the entropy. Assuming that the polarization is proportional to $\mathcal{E}$, we can write

$$\mathbf{P} = \epsilon_0 A N \mathcal{E}\ , \tag{2}$$

where ϵ_0 is the permittivity of space, and $A = (K-1)/N_a$, and K is the dielectric constant.[23] Since the independent variables in Eq. (1) are S, V, and N, the two equations can be combined to give

$$dU = T\,dS - p\,dV + (\mu + A\epsilon_0\mathcal{E}^2)dN\ . \tag{3}$$

Next, U is replaced by the Gibbs potential $G = U - TS + pV$ with the result

$$dG = -S\,dT + V\,dp + (\mu + A\epsilon_0\mathcal{E}^2)dN\ . \tag{4}$$

This can be integrated at constant T and p to give the interesting result

$$G = (\mu + A\epsilon_0\mathcal{E}^2)N\ . \tag{5}$$

We see that the term $A\epsilon_0\mathcal{E}^2$, which represents the energy of a polarizable particle in an electrostatic field, is analogous to the electrostatic field energy of a charged particle which appears as an added term in the electrochemical potential.

The Gibbs-Duhem relation is obtained by subtracting Eq. (4) from the total differential of Eq. (5):

$$N\,d\mu + NA\epsilon_0\,d\mathcal{E}^2 = -S\,dT + V\,dp\ . \tag{6}$$

From this, we obtain the rate of change of pressure with the field magnitude for a polarizable fluid:

$$(V/N)(\partial p/\partial \mathcal{E}^2)_{\mu,T} = \epsilon_0 A\ . \tag{7}$$

On combining this with the expression for the isothermal compressibility K_T, we obtain the desired relationship between volume per atom $v = V/N$ and $\mathcal{E}$:

$$(\partial v/\partial \mathcal{E}^2)_{\mu,T} = -\epsilon_0 A K_T\ . \tag{8}$$

We shall use this result in its integrated form. We will use an empirical expression $K = 9.4 - 0.052x$ to estimate K at a given composition x.[23]

B. The experimental volume contraction and compressibility

The experimental curves for the atomic volume v of the alloy versus temperature fall in a pattern which consists of two linear segments with positive slopes, separated by a range in which v decreases with T.[6] This has led to an analysis in which extensions of the linear segments represent the behavior of low- and high-temperature

forms of the liquid with atomic volumes $v_L = v_{L0} + \beta_L T$ and $v_H = V_{H0} + \beta_H T$.[9] The fraction C of the high-temperature form of the alloy is calculated from $(v_L - v)/(v_L - v_H)$. The present analysis does not require the consideration of high-temperature v_H, and we shall use the volume contraction $v_C = v_L - v$ to describe the experimental thermodynamic transition. In Fig. 2, we show curves for v_C normalized to the nominal atomic volume N_a^{-1} at compositions $x = 0$ to 50, for which we have useful data for the electronic behavior. These curves were interpolated from the original data by Thurn and Ruska with the help of an empirical formula derived in Ref. 9, and they agree well with recent measurements of Tsuchiya.[24]

We shall also need information about the isothermal compressibility K_T. Takimoto and Endo have made measurements of the adiabatic compressibility K_S in various compositions of Se_xTe_{100-x}.[7] At large x and small T, where the thermodynamic behavior is normal, K_S increases with T on curves which show little change with x. At smaller x, starting with $x = 60$, anomalous behavior occurs in which K_S goes through a maximum and then decreases with T, in a temperature range which corresponds to a negative dv/dT. This reflects the change of the average properties of the liquid due to electrostriction. Since it will be used in calculations which are very approximate, it will be sufficient for our purpose to ignore the difference between the adiabatic and isothermal compressibility, and to use the measured curve for $x = 70$ as representative of the compressibility of the low-T form of the liquid. This is described by the empirical formula $K_T = (0.00576T - 1.22) \times 10^{-5}$ bar^{-1}.

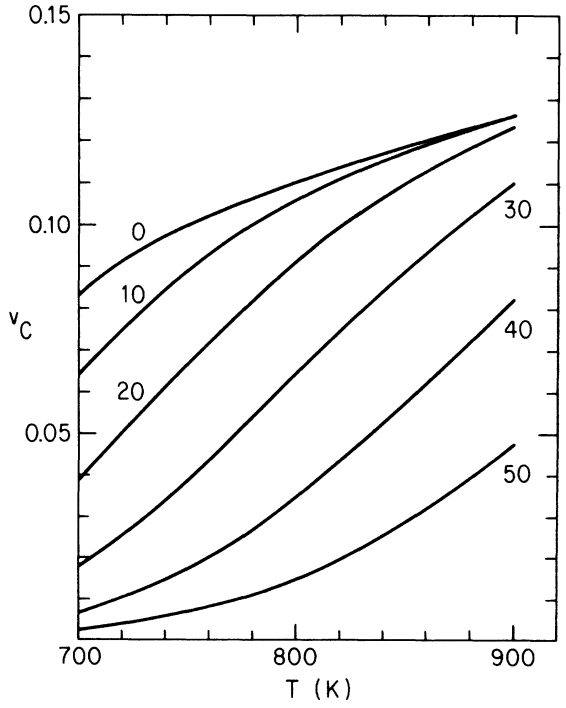

FIG. 2. Experimentally derived volume contraction v_C as a function of T for various compositions x.

III. ELECTRONIC SCREENING MODELS

A. Calculation of contraction at large hole concentrations

For reasons to be discussed later, it is very difficult to determine the electrostrictive forces with any accuracy. We shall therefore use relatively crude models which cannot be expected to yield exact results. The goal is not so much to describe the phenomenon accurately as to show that it can be expected to cause a volume change similar, both in magnitude and dependence on composition, to what is observed.

The general approach is to use a model for the distribution of charge in the vicinity of an ion in order to calculate the mean-square field $\langle \mathcal{E}^2 \rangle$. In the range of x and T for which $\mathcal{N}^+ > 0.2$, we find that a relatively simple situation occurs in which the presence of positive ions can be neglected because of their relatively low concentrations. In that case, the concentration of negative ions $\mathcal{N}^- = \mathcal{N}^+$, and the Thomas-Fermi model for the distribution $h(r)$ of a positively charged gas within a spherical volume of radius $r_0 = (3/4\pi N_a \mathcal{N}^-)^{1/3}$ can be used to determine $\mathcal{E}(r)$. The Thomas-Fermi model leads to the nonlinear differential equation

$$\frac{1}{r^2}\frac{d}{dr}r^2\frac{d\mathcal{V}(r)}{dr} = \frac{-eh(r)}{K\epsilon_0} = -(e/K\epsilon_0)(3\pi^2)^{-1}(2m/\hbar^2)^{3/2} \times [E_F - e\mathcal{V}(r)]^{3/2} , \quad (9)$$

where $\mathcal{V}(r)$ is the electrostatic potential. In all of the calculations, we assume that the hole density is zero at the site of the D^- ion, so the boundary condition for $\mathcal{E}$ at the inner radial boundary, assumed arbitrarily to be at $r_1 = (3/4\pi N_a)^{1/3}$, corresponds to a net charge of $-e$. The second boundary condition is $\mathcal{E} = 0$ at $r = r_0$. Equation (9) is solved by determining the value of E_F which causes numerical integration from r_0 to yield the correct boundary condition at $r = r_1$.[25] We then calculate the mean-square field from

$$\langle \mathcal{E}^2 \rangle = (3/r_0^3)\int_{r_1}^{r_0} [\mathcal{E}(r)]^2 r^2 \, dr . \quad (10)$$

The volume contraction v_{C1} is determined from the relation

$$v_{C1} = (K-1)K_T\epsilon_0\langle \mathcal{E}^2 \rangle , \quad (11)$$

obtained from Eq. (8).

In Fig. 3, we show the calculated curves of v_{C1} versus $\mathcal{N}^+$ for $x = 10$, 20, and 30, in comparison with the experimentally derived points v_C. It is seen that the calculated curves are too low by a factor ≈ 2, and v_{C1} has a maximum as $\mathcal{N}^+$ increases, whereas the experimental v_C curves are monotonic. The discrepancy can be ascribed to the use of macroscopic concepts in a microscopic situation. When $\mathcal{N}^+$ is large, the outer boundary r_0 is not much larger than the interatomic distance, and the model, which treats the charge as a homogeneous fluid in an electrostatic field is grossly inadequate. Since the field in-

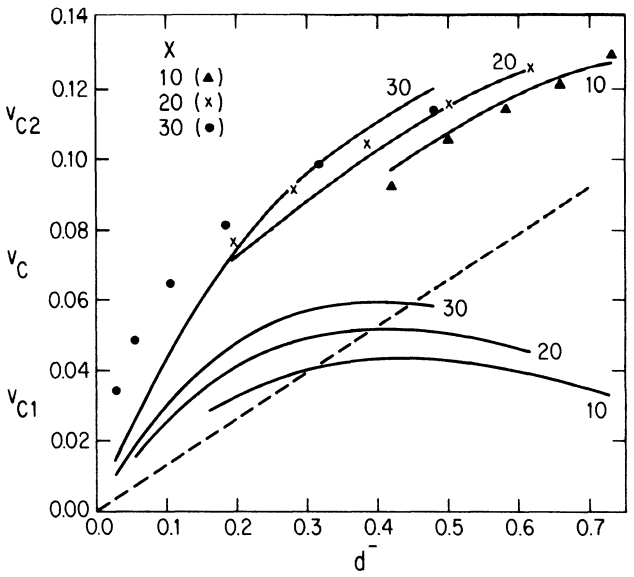

FIG. 3. Dependence of contraction on ion density d^- for $x=10$, 20, and 30. The lower set of curves is calculated values of v_{C1}. The straight line represents the correction Bd^-, and the upper curves show the calculated v_{C2} in comparison with the experimentally derived points for v_C.

creases with decreasing r, the relative contribution to the error from the integrations of Eqs. (9) and (10) is large when r is near the minimum radial distance r_1, where the atomic structure manifests itself. This type of difficulty is common to all treatments of electrostatic behavior of atoms using macroscopic concepts, and the error is very sensitive to the value chosen for r_1. On the other hand, when r_0 is much larger than r_1, the field at small r is nearly independent of the conditions at large r. Therefore the error due to the small r region near each ion can be expected to be almost constant. Similar considerations apply to the error from using the macroscopic compressibility in Eq. (8) in the small r region. This suggests a modified solution for the volume contraction of the form

$$v_{C2}=v_{C1}+Bd^- , \tag{12}$$

where B is an empirically determined constant. The term Bd^- is expected to correct much of the error generated in the vicinity of each ion due to the macroscopic formulation for the compressibility as well as the electric field. We find that a good correction is obtained with the choice $B=0.13$, as shown in Fig. 3.

B. Alloys containing positive ions

One can see in Fig. 3 that v_C tends to be larger than v_{C2} for smaller values of d^+ (<0.2). This seems to be caused by neglect of the positively charged D^+ ions. In the semiconductor range, there is evidence that the behavior of E_F is determined by the equilibrium between D^- and D^+ ions. As E_F falls below the valence-band edge in the course of the electronic transition to a metal, the holes play an increasing role in the charge distribution. We have no direct information about the positive-ion concentration d^+, so it is not possible to determine the concentrations of the two kinds of ions in the relationship

$$d^-=d^++h^+ . \tag{13}$$

In order to shed further light on the character of the semiconductor-to-metal transition, it is helpful to obtain a rough estimate of the behavior of d^+ and d^- from experimental information about v_C, by use of the electrostriction model. This can be done by using two approximations in calculating the charge distribution which have the effect of either overestimating or underestimating the ion concentrations, so that the true results can be expected to lie between these limits.

In model I, we calculate $\langle \mathcal{E}^2 \rangle$ by assuming that the screening charge of each ion is uniformly distributed on the surface of a sphere of radius $r_t=(3/4\pi N_a c_t)^{1/3}$, where $c_t=d^-+d^+$. This gives

$$\langle \mathcal{E}^2 \rangle = 3(e^2/4\pi\epsilon_0 r_t^2)^2(r_t-r_1)/r_1 . \tag{14}$$

We assume that the electrostriction due to a positive ion is the same as for negative ion, and use Eq. (12) with v_{C1} equal to the experimental v_C to calculate the total ion density c_t. This model exaggerates the value of $\langle \mathcal{E}^2 \rangle / c_t$, and therefore underestimates c_t. The values of d^- and d^+ are obtained with the help of Eq. (13), and the results for $x=30$, 40, and 50 are plotted in Figs. 4 and 5.

In model II, we neglect the electrostriction due to the positive ions, and calculate $\langle \mathcal{E}^2 \rangle$ using the same equation

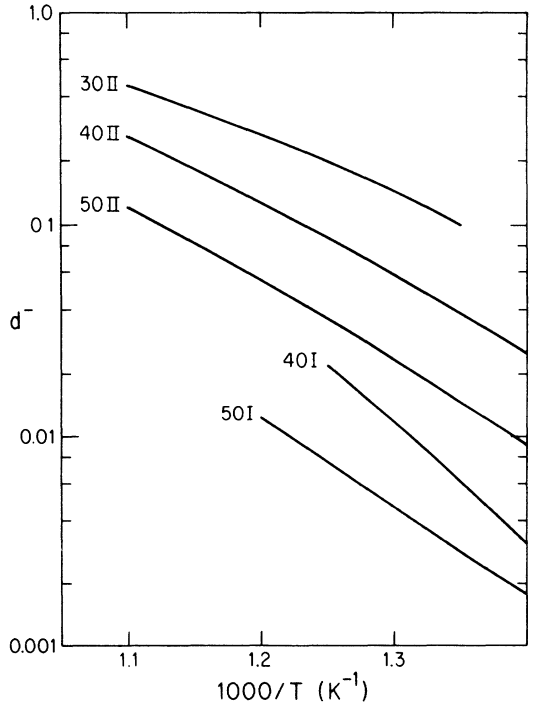

FIG. 4. Plots of the negative-ion concentrations vs T for $x=30$, 40, and 50, obtained from experimental v_C data with a model which (I) underestimates or (II) overestimates their values.

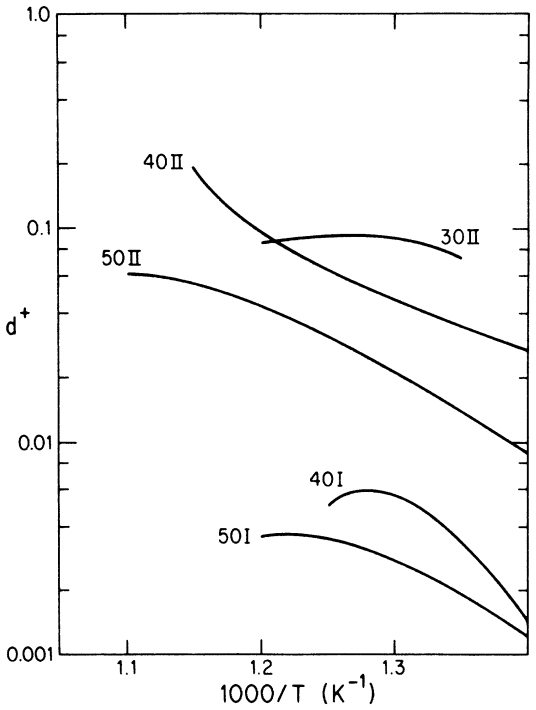

FIG. 5. Plots of the negative-ion concentrations vs T for $x=30$, 40, and 50, obtained from experimental v_C data with a model which (I) underestimates and (II) overestimates their values.

for nonlinear Thomas-Fermi screening as before (in Sec. III A), including the same assumption that $\alpha^- = \lambda^+$. A curve is plotted for $\langle \mathcal{E}^2 \rangle / \alpha^-$ versus α^- for a given composition. With the help of this curve, a consistent solution for α^- is calculated at each temperature from

$$\alpha^- = v_C / [B + (K-1) K_T \epsilon_0 \langle \mathcal{E}^2 \rangle / \alpha^-] \ . \tag{15}$$

(This is solved by iteration on α^-.) Since λ^+ is actually less than α^-, the screening of the negative ions is weaker than what is calculated, so that this model underestimates $\langle \mathcal{E}^2 \rangle$. Together with the neglect of electrostriction due to the positive ions, this results in an overestimate of α^-. The value of α^+ obtained from Eq. (13) is also overestimated.

Figures 4 and 5 show plots of α^- and α^+ obtained from both models I and II, and the true values are expected to lie somewhere between them. As x is increased and T is decreased, λ^+ becomes small. In this limit, the nonlinear Thomas-Fermi model for screening is poor because the Fermi wave vector is large compared to the distance within which the main screening occurs. For this reason, we expect model I to be more accurate in the limit of large x and small T. Model II is expected to be more accurate in the opposite end of the range, where α^+ is not yet large compared to λ^+.

IV. THERMAL GENERATION OF IONS

An ingredient which is missing from a complete description of the semiconductor-to-metal transition is a theory for the equilibrium concentration of ions as a function of T and x. We do not try to derive such a theory in this paper. But it will be useful to discuss qualitatively how screening affects the behavior of α^+ and α^- in the course of the metal transition, as indicated by the results shown in Figs. 4 and 5.

Thermal generation of ions occurs in the semiconductor range of T and x, but the coefficient of thermal expansion is normal because dc_t/dT is too small for the electrostriction to be seen above the normal thermal expansion. It is interesting to note the position of the Fermi energy when the effects of the electrostriction first become noticeable. This temperature T_L is defined to be the point at which $v(T)$ reaches a local maximum and starts to decrease.[9] For the three compositions $x=40$, 50, and 60, for which we have the necessary information, E_F is 0.1 eV below the valence-band edge.[17,26] This distance is somewhat larger than kT, and it indicates that dc_t/dT becomes large enough to make the electrostriction visible when the holes change from a Boltzmann gas to a Fermi gas. This suggests that screening by the holes plays a key role in determining the rate of generation of the ions. Other effects of the large dc_t/dT are (1) E_F shows a more rapid decrease with T above T_L,[17] and (2) the activation energy of the electrical conductivity increases from ≈ 0.8 to ≈ 1.3 eV in this range of T.[2]

To understand the role of screening in determining the equilibrium value of α^+ and α^-, we focus attention on the factor $\exp(-E_a/kT)$ which appears in the expression for the equilibrium concentration of either ion, where E_a is the energy of formation for the positive ion (E^+) or negative ion (E^-).[26] This factor is dominant in determining the magnitude of dc_t/dT. E_a can be expressed as $E_0 - E_S$, where E_0 is the energy of formation in the absence of screening, and E_S is the screening energy. Thus E_S appears in a factor $\exp(E_S/kT)$. E_S can be expressed roughly as $\frac{1}{2}e^2/4\pi\epsilon_0 K L_S$, where L_S is an average distance of the screening charge. If L_S is in angstroms, $E_S \approx 7/KL_S$ eV, and the dielectric constant K has a value in the range 7–9 for the alloys which concern us. Since $kT \approx 0.08$ eV, the screening energy is important in determining the ion concentration when $L_S < 10$ Å.

In the semiconductor range, the main charged species are the positive and negative ions, and the screening is governed by their concentrations, which are equal. The values of the parameters which determine α^+ and α^- are poorly known, but the concentrations are believed to be too large for the Debye screening model to be valid. In this case, it has been shown that a good approximation to E_S is obtained by setting $L_S = r_0$,[27] which is equal to $2/(\alpha^-)^{1/3}$ in Angstrom units. Thus, if $\alpha^- < 0.01$ in the semiconductor range, as suggested by the results in Figs. 4 and 5, $L_S > 10$ Å, and screening has little effect on the ion concentrations.

When E_F approaches the valence-band edge, λ^+ becomes large, and holes play an important part in screening. For $T > T_L$, the situation is described formally by the nonlinear Thomas-Fermi screening equation, but the solution is probably not very accurate when E_F is close to the band edge. Nonetheless, we can make estimates of

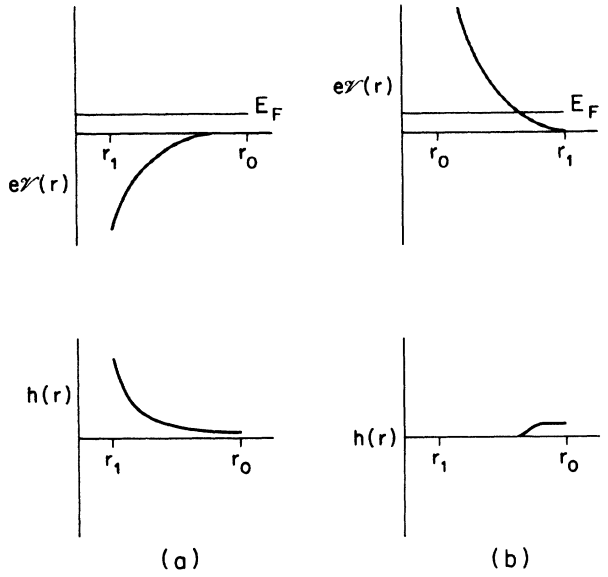

FIG. 6. Schematic plots of the radial dependence of the hole concentration $h(r)$, and potential $\mathcal{V}(r)$ in relation to the kinetic energy E_F, in the vicinity of a negative ion (a) and in the vicinity of a positive ion (b). They apply to the case where $\mathcal{A}^+$ is small, so that the kinetic energy is not very large compared to kT.

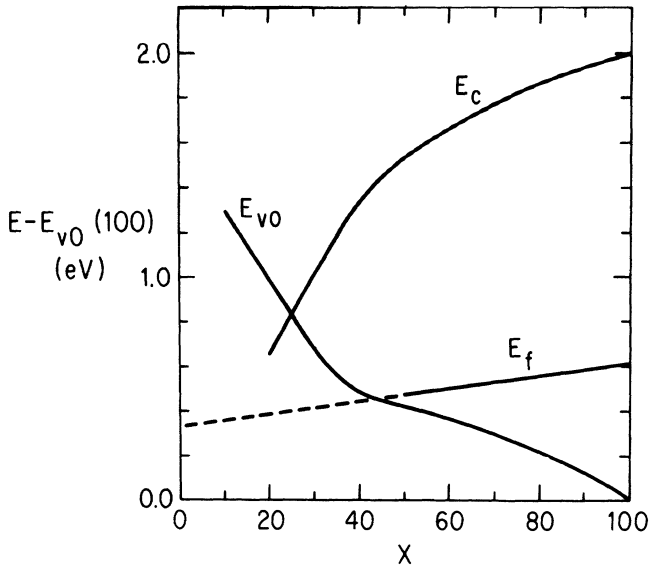

FIG. 7. The dependence of the Fermi energy E_F, the valence-band edge E_{V0}, and the conduction-band edge E_C on composition at $T=700$ K.

E_S on the basis of qualitative features of the solution, which are illustrated in Fig. 6.[26] In the vicinity of a negative ion, $E_F-e\mathcal{V}(r)$ becomes large compared to E_F, and the local hole concentration $h(r)$ is large compared to its average value. Because of the limitations of the Thomas-Fermi approximation, the solution for $h(r)$ becomes inaccurate near the inner boundary at r_1 over distances comparable to the Fermi wavelength $L_F=h/(2mE_F)^{1/2}$. However, we can expect the screening length L_S to be comparable to L_F. When the Fermi energy is in the valence band, $L_F<3$ Å, and E_S is expected to be large compared to kT. Therefore we can expect $\mathcal{A}^-$ to increase rapidly with T.

The situation is quite different for screening of the positive ions. As indicated in Fig. 6, $E_F-e\mathcal{V}(r)$ becomes negative at a relatively large distance from the ion, and $h(r)$ is reduced to zero within that distance.[26] Since $\mathcal{A}^+<\mathcal{A}^-$, that means that L_S for positive ions will remain close to r_0, and the effect of the holes will be only to make E_S for the positive ions somewhat smaller. The overall effect of the hole screening on $\mathcal{A}^+$ is more complicated because of the requirement for electrical neutrality [Eq. (13)]. At the beginning of the metal transition, when $\mathcal{A}^+\ll\mathcal{A}^+$, the rapid increase in $\mathcal{A}^-$ with T has to be accompanied by a corresponding rapid increase in $\mathcal{A}^+$, as indicated in Fig. 5. But as E_F goes deeper into the valence band, a point is reached where $\mathcal{A}^+>\mathcal{A}^+$, and the increase in $\mathcal{A}^-$ is accompanied by an increase in $\mathcal{A}^+$ rather than $\mathcal{A}^+$. It is not clear whether $\mathcal{A}^+$ reaches a maximum and then decreases, or whether it just levels off. In any case, $\mathcal{A}^+$ becomes larger than $\mathcal{A}^+$ about halfway through the metal transition, and $\mathcal{A}^-=\mathcal{A}^+$ becomes a good approximation at higher temperatures.

The rapid increase in $\mathcal{A}^-$ which characterizes the metal transition is reflected in the shifts in energy of the band edges. Experimental information on the distance of the valence-band edge from the Fermi energy $E_{V0}-E_F$ (Refs. 17 and 26) can be combined with data for the optical band gap[5] to give the distances of E_{V0} and the conduction-band edge E_C from E_F. In the semiconductor range, where most of the atoms are electrically neutral, it has been possible to calculate the behavior of E_F on a more absolute basis, in which the reference energy is taken to be the center of the valence band of liquid Se. This is shown in Fig. 7 as a solid curve for the isothermal dependence of E_F on composition, together with the corresponding curves for E_{V0} and E_C. There is no information on the absolute behavior of E_F in the composition range $x<50$, and we have extrapolated the linear behavior of E_F in the semiconductor range. The curves for E_{V0} and E_C in the metallic range correspond to this extrapolation of E_F. (The conclusions which follow do not depend on the accuracy of this assumption about E_F.) It is seen that when x decreases below 50, in the composition range of the metal transition, E_{V0} bends sharply upward and E_C bends sharply downward. The rapid rise in E_{V0} is due to the fact that the upper states of the valence band are derived from the D^- ions. Electrons which occupy these states have increasing energies due to the negative charge of the ions. These ions are at the ends of chains, and the atoms within the chains have a corresponding positive charge associated with the D^+ ions and the holes. The electron states of the conduction band correspond to regions closer to this positive charge density, and this explains the more rapid decrease in E_C.

V. SUMMARY AND CONCLUSIONS

We have derived a thermodynamic relationship between the contraction of the volume due to electrostric-

tion and the magnitude of the electric field. We have applied it in the case of alloys in which α^- can be inferred from κ^+, to calculate the contraction v_C as a function of the concentration, α^-, of negative ions. Because of the limitations of the macroscopic treatment of the relation between v_C and $\langle \mathcal{E}^2 \rangle$, and limitations of the models for the dependence of $\langle \mathcal{E}^2 \rangle$ on α^-, the derived relationship between v_C and α^- was not very accurate, but much of the error could be corrected by means of constant increment to v_C for each ion due to interactions close to the ion. These results show that electrostriction can be expected to cause a volume contraction comparable to what is observed, and the model provides an approximate quantitative description. For the range of x and T where the presence of positive ions prevents the determination of α^- from κ^+, the model was used to find curves for the ion concentrations versus T which limit the possible range of values. We then explained how the screening of the ions by the holes can be expected to influence the thermal generation of ions to cause the behavior shown in Figs. 4 and 5.

In all of this, the most striking limitation of our models comes from the difficulty in describing the electrostatic interactions due to charge distributions on the scale of the size of an atom. This seems to be a basic problem which can be only addressed by a full scale quantum-mechanical treatment, comparable to what is done in the theory of chemical bonding. Rough estimates based on the macroscopic law of force on a polarizable atom indicate that the force on such an atom in contact with an ion is comparable to the force between oppositely charged ions at the same separation distance.

This is relevant to the question of reconciling the electrostriction hypothesis with experimental structural information on Se-Te alloys. For both the Raman and the diffraction studies, evidence for deviations from the twofold bonding structure of Se that occurs at small x has been identified with the more clearly defined behavior of pure Te. In recent years, Tourand's conclusions about the pair correlation function have been criticized and revised by Enderby and Barnes.[28] This revision indicates that there is disorder in the nearest-neighbor (NN) shell, which seems to be consistent with the expected behavior due to electrostriction. If we use the hole concentration derived for $x=10$ at higher temperatures as a typical value for liquid Te, $\kappa^+=0.7$, so that the typical molecule is a chain of three atoms. The two chain ends carry negative charge, and the midchain atoms are positively charged. One would expect a midchain atom to be strongly attracted to the chain end of one or more neighboring molecules. As a result, the atoms in the NN shell beyond the two that are covalently bonded would be in a disordered arrangement.

The experimental Raman spectra clearly show a qualitative change in bonding between alloys with $x \leq 20$ and larger values of x.[14] It should be noted that these results reflect the situation at the lowest temperatures, since the decreasing phonon lifetime washes out the spectra at higher T. Magaña and Lannin have noted a qualitative similarity of the spectra for Te with amorphous As and P, but a definitive identification of the structure has not been made.[15] Our data show that $\alpha^- > 0.5$ for $x \leq 20$, so that there is a large concentration of D^- ions in close contact with atoms which are otherwise twofold bonded. This can be expected to modify the Raman spectrum from the one which characterizes the twofold bonded chain molecules at larger x. In order to explain the observed effect of optical polarization on the Raman spectra, it is necessary that there be an interaction between the extra coupling of an atom to the neighboring ion and the covalent bond coupling to the chain neighbors.[29] We think that this is to be expected as the result of a strong perturbation of the bonding orbitals when the atom is in contact with an ion.

ACKNOWLEDGMENTS

This research has been supported by the National Science Foundation under Grant No. DMR-83-20547.

[1]J. C. Perron, Adv. Phys. **16**, 657 (1967).
[2]M. Cutler, *Liquid Semiconductors* (Academic, New York, 1977).
[3]N. F. Mott and E. A. Davis, *Electronic Processes in Non-Crystalline Materials*, 2nd ed. (Clarendon, Oxford, 1979).
[4]J. A. Gardner and M. Cutler, Phys. Rev. B **14**, 4488 (1976).
[5]L. A. Silva and M. Cutler (unpublished); Larry A. Silva, Ph.D. thesis, Oregon State University, 1989.
[6]H. Thurn and J. Ruska, J. Non-Cryst. Solids **22**, 331 (1976).
[7]K. Takimoto and H. Endo, Phys. Chem. Liq. **12**, 141 (1982).
[8]S. Takeda, H. Okazaki, and S. Tamaki, Phys. Rev. B **31**, 7452 (1985).
[9]M. Cutler and H. Rasolondramanitra, in *Localization and Metal-Insulator Transitions*, edited by H. Fritzsche and D. Adler (Plenum, New York, 1985), p. 119.
[10]R. Bellisent, Nucl. Instrum. Methods **199**, 289 (1982).
[11]M. Cutler, Phys. Rev. B **20**, 2981 (1979).
[12]G. Tourand, J. Phys. (Paris) **34**, 937 (1973).
[13]G. Tourand, Phys. Lett. **54A**, 209 (1975).
[14]J. R. Magaña and J. S. Lannin, Phys. Rev. B **29**, 5663 (1984).
[15]J. R. Magaña and J. S. Lannin, Phys. Rev. Lett. **51**, 2398 (1983).
[16]B. Cabane and J. Friedel, J. Phys. (Paris) **32**, 73 (1971).
[17]S. S. Kao and M. Cutler, Phys. Rev. B **37**, 10 581 (1988).
[18]R. J. Hodgkinson, Philos. Mag. **23**, 673 (1971).
[19]M. H. Cohen and J. Jortner, J. Phys. (Paris) Colloq. **35**, C4-345 (1974).
[20]Y. Tsuchiya and E. F. W. Seymour, J. Phys. C **15**, L687 (1982).
[21]H. Endo, J. Non-Cryst. Solids **59-60**, 1047 (1983).
[22]R. W. Gurney, *Ionic Processes in Solution* (McGraw-Hill, New York, 1953), p. 188.
[23]The parameter A resembles the polarizability per particle $\alpha = d(\mathbf{P}/N_a)/d\mathcal{E}_{\text{loc}}$, but differs from it in being a derivative with respect to the global field $\mathcal{E}$ rather than the local field $\mathcal{E}_{\text{loc}}$. If the geometry of the particle is modeled by a sphere,

$A=\alpha/[1-(N_a\alpha/3)]$. In using the macroscopic dielectric constant K to calculate A, we ignore the fact that there are two species of atoms with different polarizabilities, and treat the particles as if they have a single polarizability which is calculated from K as indicated. We shall use an empirically derived estimate for K, which is based on an interpolation of data for solid Se and Te, with a correction for the change in volume on melting. That result was subsequently modified somewhat to put it into accord with data for the index of refraction of the liquid alloys in R. Fainshtein and J. C. Thompson, Phys. Rev. B **27**, 5967 (1983).

[24]Y. Tsuchiya, J. Phys. Soc. Jpn. **57**, 3851 (1988).
[25]M. Cutler, Phys. Rev. **181**, 1102 (1969).
[26]S. S. Kao and M. Cutler, Phys. Rev. B **38**, 9457 (1988).
[27]M. Cutler, Philos. Mag. **49**, 83 (1984).
[28]J. E. Enderby and A. C. Barnes, Rep. Prog. Phys. (to be published).
[29]We wish to thank J. S. Lannin, who pointed this out to us.